Journal of Applied Research in Science and Humanities

GEOLOGICAL AND MINERALOGICAL STUDIES OF THE QUATERNARY SEDIMENTS IN GIZA, EGYPT

Aya Ashraf, Esraa Salem, Salma Nabil, Shrouk Saad, Soad Nashed

Supervisor: Dr.Omnia El Sayed Zaki, Lecturer of geology

Ain Shams University, Cairo, Faculty of Education, Department of Biological and Geological Sciences.

Abstract

Extensive Quaternary deposits are exposed in the Kafr El Gebel region, situated south of the Sphinx in Giza, Egypt.

A selection of ٥ stratigraphic sections has been made for examination and sampling. To look into the mineralogical and sedimentological features of the Quaternary sediments, ٣٠ samples were gathered. The examined sands are primarily medium to coarse, very well sorted to poorly sorted, and mostly near symmetrical skewed with mesokurtic to leptokurtic features, according to the statistical grain size parameters. The textural features strongly imply that the braided river's fluvial conditions were most likely the primary determinants influencing the movement and accumulation of the sediments under investigation. The majority of the light minerals in the sand under investigation are quartz, with a trace proportion of feldspar.

The Quaternary sediments' non–opaque heavy mineral assemblages are typified by the prevalence of pyroxene, rutile, garnet, amphiboles, epidote, zircon, tourmaline, staurolite, and kyanite. A few samples contain andalusite, titanite, and monazite. The ZTR index's low values

indicate that these sediments are mineralogically immature. These sediments' rich mineral assem blage suggests a range of likely source rock types, including volcanic, metamorphic, and sedimentary rocks.

Key Words:

Grain size, Heavy minerals, Quaternary sediments, Giza

Introduction:Sedimentation of detrital sediments and rocks is controlled by major parameters such as source rock composition, chemical weathering, and mechanical disintegration (eg. Johnsson, 1993; Abuodha, 2003; Weltje and von Eynatten, 2004). Mineralogical and geochemistry properties of detrital sediments data determine the evidence of the composition of the source rocks, deposition environment and transport factors (Friedman, 196; Folk, 1966; Lario et al., 2002; Garzanti et al., 2009; Alharbi et al., 2016). Clarification of these data aids in disentangling of depositional environment and elucidating transporting medium nature and dynamics (Mycielska– Dowgiałło and Ludwikowska– Kędzia, 2011). The mineralogical composition of detrital sediment and heavy minerals (HM) assemblage is considered an indicator of the source of the sediment (Nechaev and Isphording, 1993; Morton and Hallsworth, 1994; Wong, 2002). Heavy minerals assemblages in detrital sediments are controlled by specific gravity, stability during transportation and weathering, source rock mineralogical composition and mineral shape and size. During fluvial transport, chemical weathering reduces the heavy of mineral diversity (Johansson and Meade, 1990; Savage and Potter 1991; Garzanti et al., 2019). The floods of the Nile River led to the transfer of detrital sediments from regions with different climates, geomorphology, and foundation geology to the floodplains in Egypt for thousands of years. (Foucault and Stanley, 1989; Said, 1993).The oldest delta of The River Nile is recorded near the Fayoum and is dated in the Eocene (38–35 Ma) (Salem, 1976). The delta began to decline towards the north, and the Tethys Ocean receded and deposited in its current offshore location in the Oligocene epoch (30 Ma) (Craig et al., 2011). As a result of the shoulders uplift of the Ethiopian Rift with associated increased precipitation and erosion, MacGregor (2012) suggested that during the late Pliocene and early Pleistocene, there was an increase in the rate of sedimentation in the cone of the Nile Delta. At the beginning of the 20th century, the study of alluvial deposits

in the Nile Valley and Delta began. These studies have a long history, and most of these studies focused on the Nile sediments in the Pleistocene epoch in Upper Egypt (Butzer and Hansen, 1968; Said, 1981, 1993). Numerous geological and archeological studies have been conducted on the Holocene sediments of the Nile floodplain (e.g. Wendorf and Schild, 1976). Shukri's groundbreaking work in 1950 marked the beginning of investigations into the mineralogy of Nile sediments, and it paved the way for numerous in-depth research on the heavy minerals that make up the Nile River's sediments (e.g., Shukri, 1950; Hassan, 1976; Foucault and Stanley, 1989; Frihy et al. 1995). The primary component of clay, kaolinite minerals, is abundant in the Nile sediments, according to studies done on clay minerals and the geochemistry of the sediments. (For example, Siegel et al., 1995; Stanley and Wingerath, 1996; Dawood and Abd El Naby, 2012).

STUDY AREA

The study area "Kafr El Gebel" is situated on the west bank of the Nile River, next to the large delta of it. It is across from Cairo, the capital of modern-day Egypt, and is about 8 km south of Abu Rawash and 17 km north of Saqqara. The Sphinx is located 19 km to the south of the study region.

2. SAMPLING AND ANALYTICAL PROCEDURES

Carefully measured, documented, and sampled were five stratigraphic sections (Fig. 1). Thirty samples total, encompassing the Late Pleistocene (3 samples), Middle Pleistocene (11 samples), Early Pleistocene (13 samples), and Holocene (3 samples), were taken from the study region.

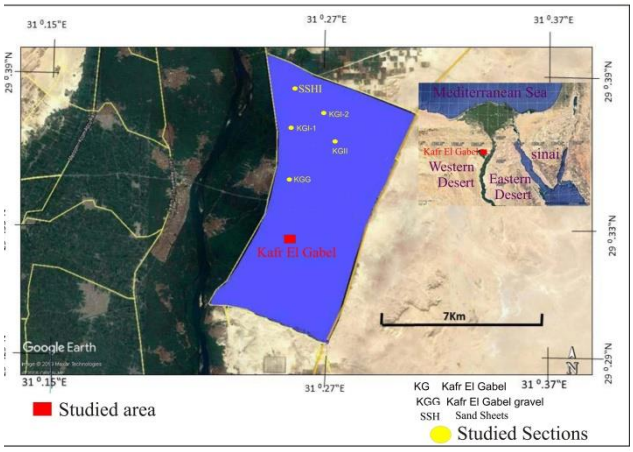

Figure (1): Location map of the study area

Dry sieving was used to make the grain-size analysis. A Ro-Tap shaking machine was used to sift 100 g of each sample for 20 m. Standard mesh sieves with a set of sizes of 0, 1, 2, 3, and 4 Ø were used.

The cumulative curves were used to determine the textural parameters according to Folk and Ward (1957), using the following phi values: Ø 5, Ø 16, Ø 25, Ø 50, Ø 75, Ø 84, and Ø 95.

A PANanalytical X-Ray Diffraction equipment type X'Pert PRO with a monochromator, Cu-radiation (ɣ=1.542 Å) at

40 Kv, 40 mA, and scanning speed of 0.03°/sec was used to investigate representative bulk materials mineralogically utilizing X-ray diffraction (XRD). Using bromoform (specific gravity 2.85), a heavy liquid, heavy minerals have been isolated from 63–125 μm and 125–250 μm (fine and very fine sand-size fractions) using a conventional procedure (Galehouse, 1971; Mange and Maurer, 1992). The heavy portion that had been separated was cleaned using acetone and ethyl alcohol before being adhered to a glass slide using Canada balsam. For every heavy mineral mount, more than 300 grains have been counted in the sample. Using an Olympus polarized microscope, the heavy and light minerals were distinguished (Mange and Maurer, 1992). Grain percentages were used to calculate the mineralogical composition. Following Hubert (1962), the ZTR index (% of Zircon Tourmaline–Rutile/Non-Opaques) was computed. The Olympus Polarized microscope was used to analyze the thin slices of the collected gravel.

4. Results of Research

Grain-size analysis

Tables 1 and 2 provide the grain-size distributions of the sediment samples under study together with their characteristics, which were determined using Folk and Ward's (1957) formula. The ternary diagram of gravel, sand, and mud (Fig. 2) is used to plot the collected particle size data (Folk, 1954). In the sediment samples under study, the most prevalent particle size is the sand fraction. According to the findings, the Early Pleistocene sediments are divided into 6.67% gravelly sand and 93.33% sand. The Middle Pleistocene sediments have three different classifications: 63.64% sand, 13.64% gravelly sand, and 22.72% sandy gravel. 3.33% of the Late Pleistocene sediments are gravelly sand and 66.67% of the sediments are sand. Conversely, the Holocene deposits are divided into 11.11% gravelly sand and 88.89% sand. Additionally, the Pleistocene sediments are generally coarser than Holocene sediments.

Two modes of conveyance are recognized for the examined Pleistocene and Holocene sediments. The saltation population was considered the main population of transportation mechanism with small contributions from rolling populations (Fig. 3). The estimated grain size characteristics (Folk and Ward, 1957) showed that there is a considerable amount of variance in the primary size and sorting of the sediments under study, especially in skewness and kurtosis (Fig. 4). The high energy conditions that remove the small-sized sediments were indicated by the presence of coarse-grained components in the sediments under study. Their riverine and fluvial provenance was confirmed by the observed fluctuation of the predicted grain size parameters and the preponderance of rolling and saltation populations. It exposed the sliding and saltation agents of the braided channels' point bars (Mahmoud, 2018). The results of the grain size analysis indicate the high energy current of braided channels.

Table 1: Percentages of the various size fractions in the samples and their textural nomenclature

Age	Sample No.	Gravel %	Sand %	Mud %	Nomenclature (Folk, 1954)
Early Pleistocene	1	7.46	92.31	0.23	Sand
	2	21.17	78.36	0.47	Gravelly Sand
	3	7.23	92.52	0.24	Sand
	4	4.35	94.57	1.08	Sand
	5	2.60	95.73	1.67	Sand
	6	2.89	94.82	2.29	Sand
	7	0.56	94.41	5.04	Sand
	8	1.05	96.99	1.96	Sand
	9	0.07	96.97	2.96	Sand
	10	1.01	94.62	4.38	Sand
	11	3.05	95.00	1.95	Sand
	12	3.13	93.98	2.88	Sand
	13	2.17	97.30	0.53	Sand
Middle Pleistocene	14	9.71	87.12	3.17	Gravelly Sand
	15	5.33	94.37	0.31	Sand
	16	51.02	47.98	1.00	Sandy Gravel
	17	1.99	97.62	0.40	Sand
	18	0.14	99.39	0.47	Sand
	19	1.84	97.89	0.27	Sand
	20	2.70	97.04	0.25	Sand
	21	7.47	92.39	0.14	Sand
	22	25.52	73.99	0.49	Gravelly Sand
	23	1.80	98.03	0.17	Sand
	24	3.45	96.49	0.06	Sand
Late Pleistocene	25	11.99	87.32	0.70	Gravelly Sand
	26	0.06	99.60	0.34	Sand
	27	4.18	95.51	0.30	Sand
Holocene	28	4.59	95.04	0.37	Sand
	29	3.88	95.52	0.60	Sand
	30	5.51	94.13	0.36	Sand

.

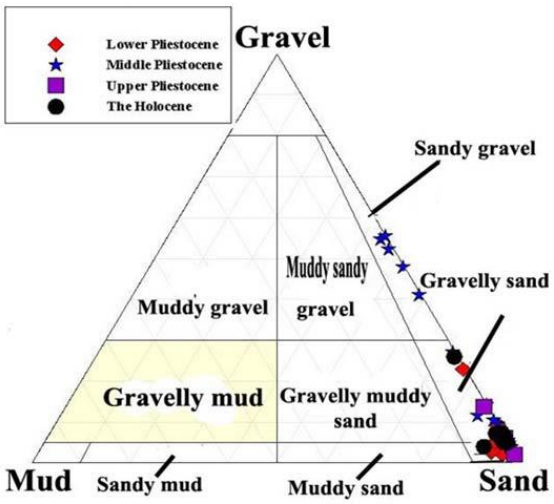

Figure 2: Plotting of the studied sediments on the ternary diagram proposed by Folk (1954)

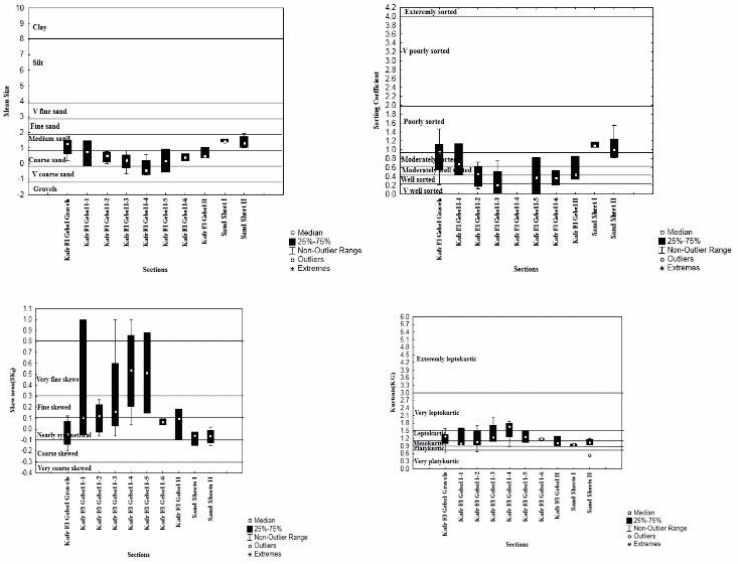

Figure 4: Boxplots of mean size, sorting coefficient, skewness and kurtosis of the studied sediments.

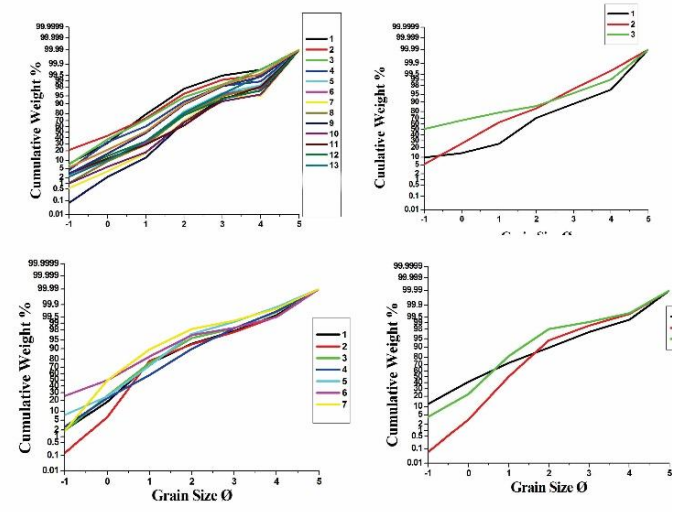

Figure 3: Probability cumulative curves of the studied sediments samples

Table 2: Grain size parameters of the studied sediment samples

Age	S.No.	Mean size (Mz)		Standard deviation (σ)		Skewness (SK)		Kurtosis (KG)	
Early Pleistocene	1	0.37	Coarse Sand	0.28	V well sorted	-0.05	Nearly symmetrical	1.01	Mesokurtic
	2	0.17	Coarse Sand	0.21	V well sorted	0.06	Nearly symmetrical	0.66	V platykurtic
	3	0.40	Coarse Sand	0.37	Well sorted	0.05	Nearly symmetrical	0.91	Mesokurtic
	4	0.63	Coarse Sand	0.55	Moderately well sorted	0.07	Nearly symmetrical	0.85	Platykurtic
	5	1.27	Medium Sand	0.93	Moderately sorted	-0.20	Coarse skewed	1.39	Leptokurtic
	6	1.30	Medium Sand	0.97	Moderately sorted	-0.15	Coarse skewed	1.30	Leptokurtic
	7	1.70	Medium Sand	1.47	Poorly sorted	0.09	Nearly symmetrical	1.52	V leptokurtic
	8	1.37	Medium Sand	1.08	Poorly sorted	-0.04	Nearly symmetrical	1.35	Leptokurtic
	9	1.77	Medium Sand	1.46	Poorly sorted	0.12	Fine Skewed	1.32	Leptokurtic
	10	1.73	Medium Sand	1.44	Poorly sorted	0.07	Nearly symmetrical	1.60	V leptokurtic
	11	1.50	Medium Sand	1.12	Poorly sorted	-0.14	Coarse skewed	1.09	Mesokurtic
	12	1.27	Medium Sand	1.01	Poorly sorted	-0.10	Nearly symmetrical	1.29	Leptokurtic
	13	1.23	Medium Sand	0.95	Moderately sorted	-0.10	Nearly symmetrical	1.30	Leptokurtic
Middle Pleistocene	14	1.47	Medium Sand	1.13	Poorly sorted	-0.05	Nearly symmetrical	1.61	V leptokurtic
	15	0.80	Coarse Sand	0.68	Moderately well sorted	0.11	Fine Skewed	1.01	Mesokurtic
	16	-0.13	V coarse Sand	0.44	Well sorted	1.00	Strongly fine skewed	0.94	Mesokurtic
	17	0.63	Coarse Sand	0.58	Moderately well sorted	0.12	Fine Skewed	1.49	Leptokurtic
	18	0.73	Coarse Sand	0.72	Moderately sorted	0.23	Fine Skewed	1.71	V leptokurtic
	19	0.53	Coarse Sand	0.46	Well sorted	0.07	Nearly symmetrical	1.07	Mesokurtic
	20	0.77	Coarse Sand	0.62	Moderately well sorted	-0.03	Nearly symmetrical	0.94	Mesokurtic
	21	0.47	Coarse Sand	0.35	Well sorted	-0.07	Nearly symmetrical	1.04	Mesokurtic
	22	0.00	Coarse Sand	0.12	V well sorted	0.14	Fine Skewed	0.68	Platykurtic
	23	0.10	Coarse Sand	0.18	V well sorted	0.27	Fine Skewed	1.18	Leptokurtic
	24	0.13	Coarse Sand	0.17	V well sorted	0.12	Fine Skewed	1.09	Mesokurtic
Late Pleistocene	25	0.37	Coarse Sand	0.44	Well sorted	0.18	Fine Skewed	0.92	Mesokurtic
	26	1.03	Medium Sand	0.86	Moderately sorted	0.10	Fine Skewed	1.02	Mesokurtic
	27	0.47	Coarse Sand	0.33	V well sorted	-0.10	Nearly symmetrical	1.28	Leptokurtic
Holocene	28	1.43	Medium Sand	1.09	Poorly sorted	-0.03	Nearly symmetrical	0.91	Mesokurtic
	29	1.60	Medium Sand	1.17	Poorly sorted	-0.15	Coarse skewed	0.96	Mesokurtic
	30	1.40	Medium Sand	1.05	Poorly sorted	-0.06	Nearly symmetrical	0.98	Mesokurtic

Gravel Analysis

The investigated thin sections revealed that most of the gravels are of sedimentary origin besides a few igneous and metamorphic clasts (Fig 5).

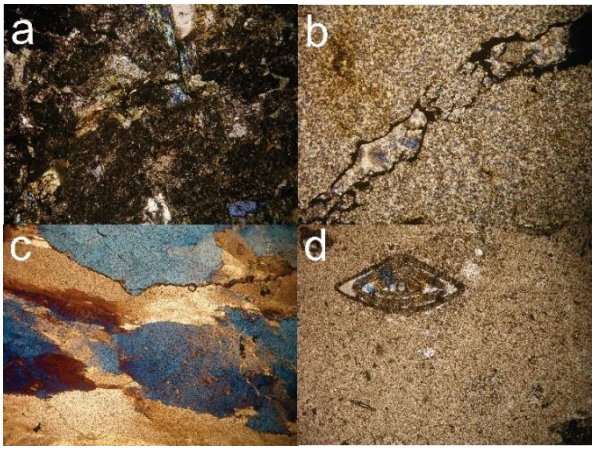

Figure 5: Photomicrographs illustrate the various compositions of gravel, (a) altered volcanic rock; (b) chert; (c) deformed quartz in metamorphic rock; and (d) limestone.

Mineralogy

Using the XRD method, the initial phase of the mineralogical examination was performed on a few chosen bulk samples. The data from bulk samples (Fig. 6) demonstrate the non–silicate minerals are gypsum and calcite, while the silicate minerals are quartz, albite, and illite. In the examined samples, the heavy index percentage falls between 1.57% and 18.68% (average 3.88%), while the light index percentage falls between 81.32 and 98.43% (average 96.12%). Up to 98% of the light portion of the samples under study is quartz grains, with a small percentage of modified feldspars. The investigated sediment samples' heavy mineral composition contains opaque and non–opaque heavy minerals.

The opaque minerals that could not be successfully separated effectively in the present study are magnetite, ilmenite, hematite, and limonite (Shukri, 1950; Hassan, 1976). In the Early Pleistocene, Middle Pleistocene, Late Pleistocene, and Holocene layers, the average percentage of these minerals is 62.29, 65.29, 64.31, and 55.91%, respectively (Table 3). In terms of mineral species, the non–opaque heavy mineral assemblages from the Pleistocene and Holocene are extremely similar. These minerals are Pyroxene, amphiboles, epidote, zircon, tourmaline, rutile, garnet, staurolite, and kyanite. A few samples contain andalusite, titanite, and monazite. They are divided into three categories in the current study: unstable, metastable, and ultrastable.

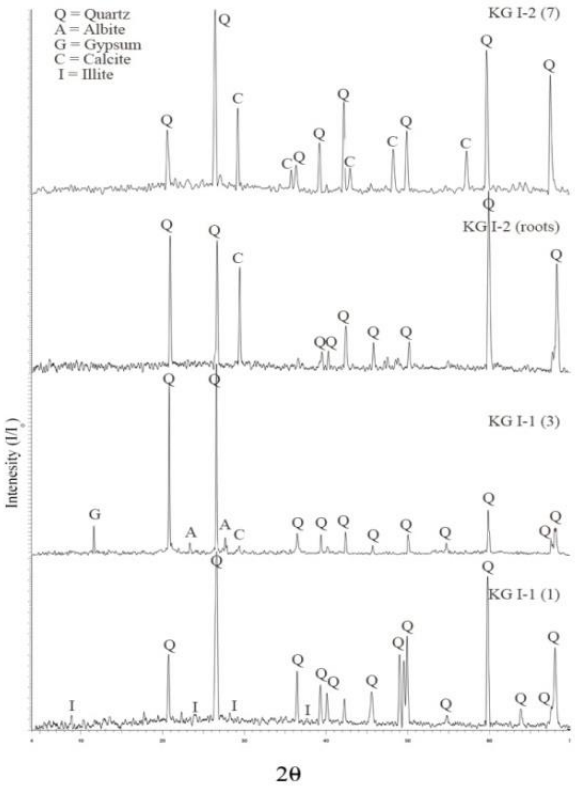

Figure 6: X-ray diffractograms of bulk samples.

Unstable heavy minerals include amphiboles and pyroxenes. Tremolite and hornblende serve as the primary representatives of the Amphibole group in the sediments under study. Hornblende is characterized by distinct cleavage and a green color (Fig. 7). The primary representative of pyroxenes is augite. The pyroxene grains exhibit fractures and inclusions, range in color from colorless to green, and are subrounded to subangular, fresh to slightly changed (Fig. 7). Because amphibole and pyroxene are unstable minerals, their occurrence is typically restricted to younger sediments (Pettijohn, 1941, 1975; Morton, 1985).

Among the metastable heavy minerals are garnet, kyanite, staurolite, and epidote. Most of the epidote grains have a yellowish–green prismatic appearance (Fig. 7). The garnet is primarily a pale pink, yet it can also be colorless. Some of these grains are spherical to subangular and they are broken. A handful of the garnet grains that have been observed have pitted grain surfaces, and the majority of them contain inclusions (Fig. 7). Subangular grains of staurolite are yellowish brown and pale yellow in hue; certain grains include inclusions (Fig. 7). The kyanite grains that have been found are cleavable prismatic grains, elongated, and colorless (Fig. 7).

Ultrastable heavy minerals of the studied sediments include zircon, tourmaline, and rutile. The most common mineral in this group is zircon. It appears as spherical, colorless, prismatic rounded and surrounded grains. The zircon grains always have inclusions and some are fractured (Fig. 8). The visible tourmaline grains are brown. They are sub–rounded and very pleochroic prismatic; occasionally, they are observed as euhedral gains (Fig. 8). Rutile grains have a short prismatic shape with subrounded corners, a broad and thick border, and a deep red or reddish–brown color (Fig. 8).

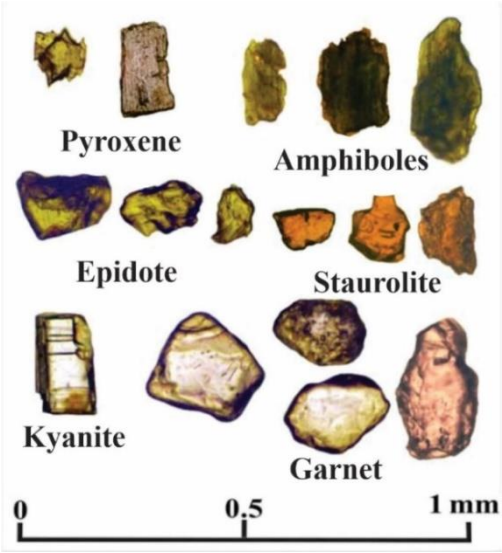

Figure 7: Photomicrographs of unstable and metastable heavy minerals

Figure 8: Photomicrographs of ultrastable heavy minerals

Table 3: Relative abundances of heavy minerals from the studied sediments

Age	S.No	Op	Py	Am	Zrn	Tou	Rut	Ept	Gar	Sta	Ky	Others	ZTR
Early Pleistocene	1	59.59	8.72	4.36	3.20	3.49	0.87	13.95	2.91	1.45	0.87	0.58	23.42
	2	64.67	6.31	4.42	3.15	2.84	0.95	14.20	1.26	1.26	0.63	0.32	24.72
	3	65.35	6.08	5.17	2.74	3.95	1.52	10.94	0.30	2.74	0.91	0.30	31.40
	4	60.56	7.14	5.28	0.93	2.17	1.24	19.25	2.17	0.93	0.00	0.31	12.50
	5	60.98	9.15	5.18	2.74	3.05	1.52	13.11	2.44	1.83	0.00	0.00	23.08
	6	62.69	7.46	5.97	4.48	2.69	1.19	12.84	1.19	0.60	0.60	0.30	29.17
	7	60.90	8.33	5.77	2.56	2.24	0.32	16.35	1.28	0.64	0.96	0.64	15.38
	8	57.88	8.36	4.50	3.22	2.89	1.93	17.04	2.57	0.96	0.64	0.00	23.58
	9	53.68	9.20	4.91	2.45	3.07	1.23	22.09	1.23	1.53	0.61	0.00	17.05
	10	66.77	7.42	4.75	2.97	2.67	1.19	11.28	1.19	1.19	0.30	0.30	26.14
	11	67.07	6.71	5.49	2.74	3.35	1.52	11.28	0.61	0.61	0.61	0.00	30.12
	12	65.22	9.32	4.66	2.48	1.86	1.24	11.80	1.55	0.93	0.62	0.31	19.35
	13	62.89	8.18	3.77	2.83	2.52	2.20	13.52	2.20	0.63	0.63	0.63	26.09
	Ave.	**62.17**	**7.87**	**4.94**	**2.80**	**2.83**	**1.30**	**14.43**	**1.60**	**1.25**	**0.56**	**0.28**	**23.23**
Middle Pleistocene	14	62.15	2.76	6.63	8.29	5.25	1.38	11.05	1.10	0.28	0.55	0.55	66.67
	15	48.54	6.07	9.71	7.28	7.04	1.21	17.96	0.73	0.73	0.49	0.24	43.54
	16	65.90	4.30	7.45	4.87	2.29	2.58	10.89	0.29	0.57	0.29	0.57	40.96
	17	78.53	4.19	3.40	1.83	1.57	0.79	8.64	0.52	0.26	0.26	0.00	24.24
	18	83.09	2.97	3.26	0.59	0.89	0.59	6.53	0.89	0.59	0.30	0.30	14.29
	19	66.27	7.83	3.92	3.31	2.11	1.51	12.95	0.90	0.90	0.30	0.00	25.84
	20	78.37	4.70	2.82	2.51	0.94	1.25	8.15	1.25	0.00	0.00	0.00	27.78
	21	5.53	7.55	3.32	1.21	0.60	0.00	10.88	0.30	0.00	0.60	0.00	8.00
	22	77.13	7.98	2.39	1.33	1.06	0.53	8.78	0.80	0.00	0.00	0.00	14.67
	23	67.28	6.12	5.50	2.75	2.14	0.61	13.46	0.92	0.61	0.00	0.61	20.69
	24	53.41	7.42	5.93	4.45	3.56	0.89	21.07	1.19	1.48	0.30	0.30	23.81
	Ave.	**8.72**	**5.62**	**4.93**	**3.49**	**2.49**	**1.03**	**11.85**	**0.80**	**0.49**	**0.28**	**0.23**	**28.22**
Late Pleistocene	25	6.73	9.46	3.15	2.87	2.29	1.72	20.06	0.29	0.57	2.58	0.29	19.05
	26	65.77	6.85	3.57	2.68	1.49	1.19	13.69	2.38	2.08	0.00	0.30	18.75
	27	70.43	5.65	2.96	2.96	1.08	0.81	14.25	0.81	0.81	0.00	0.27	19.78
	Ave.	**64.31**	**7.32**	**3.23**	**2.83**	**1.62**	**1.24**	**16.00**	**1.16**	**1.15**	**0.86**	**0.28**	**19.19**
Holocene	28	7.36	15.71	5.74	3.24	2.99	1.25	11.22	1.75	0.50	0.25	0.00	21.28
	29	62.94	15.38	2.80	3.26	2.80	1.40	10.02	0.70	0.23	0.23	0.23	25.40
	30	63.19	17.31	3.02	2.20	1.92	1.10	9.62	1.10	0.27	0.27	0.00	16.52
	Ave.	**61.16**	**16.13**	**3.8**	**2.9**	**2.57**	**1.25**	**10.28**	**1.18**	**0.33**	**0.25**	**0.07**	**21.06**

Py= Pyroxene, **Am= Amphiboles**, **Ru= Rutile**, **St= Staurolite**, **Ga= Garnet**, **Ep= Epidote**, **Tou= Tourmaline**, **Ky= Kyanite**, **Zrn= Zircon**, **Others= Sillimanite + Andalusite + Titanite**, **Op= Opaque**.

5. Interpretation of Results

Compositional and mineralogical data show a variety of broad geographical patterns.
The fact that sediments were deposited on a floodplain, which validated the nature of the cumulative curves, was one of the signs explaining the sediment's structural features.
Pleistocene and Holocene grain size characteristics of the identified sedimentary structures indicate high sedimentation under medium–to–high energy of the braided river.
The majority of the heavy mineral assemblages in the Pleistocene and Holocene strata are similar, indicating that their provenances were identical throughout their deposition. This assemblage suggests several likely source rock types, such as metamorphic, igneous, and sedimentary.
The heavy minerals are often slightly rounded, and they frequently exist as angular to subangular grains.
The majority of the examined samples exhibit pyroxene and amphibole enrichment, indicating the significance of basement rocks in their distribution. The origin of these deposits is verified by the prismatic and rounded grains of ultra–stable minerals present. The Ethiopian volcanic terrain's high pyroxene composition was caused by erosion (Foucault and Stanley, 1989) and may be from neighboring Oligocene basalt sheets.
Andalusite, garnet, kyanite, staurolite, and epidote are signs of a metamorphic source (Milner et al. 1962).

6. Conclusion

Measurements are made of the grain size analysis and sedimentary structure in the Quaternary strata of the Kafr El Gebel area, both quantitatively and qualitatively. The majority of them exhibit a large–scale planner wedged shape cross bedding of coarse to very coarse sand grains, which are carried by traction and saltation agents. This suggests that the defunct network braided Nile channels had a medium to high energy current. In terms of mineral species, the non–opaque heavy mineral assemblages from the Pleistocene and Holocene are extremely similar.
These include garnet, rutile, kyanite, amphiboles, zircon, tourmaline, pyroxene, and staurolite.
A few samples contain andalusite, titanite, and monazite. The low ZTR index values indicate that these sediments are mineralogically immature. These sediments' rich mineral assemblage suggests a range of likely source rock types, including volcanic, sedimentary, and metamorphic rocks.

Acknowledgment

All thanks and appreciation for the great efforts that were made to produce the graduation research in this brilliant manner.
Special thanks to Dr. Omnia El–Sayed for her efforts and cooperation with us throughout the past period.

References and Sources

Abuodha, J. O. (2003): Grain size distribution and composition of modern dune and beach sediments, Malindi Bay coast, Kenya. J. Afr. Earth Sci. 36:41-54.

Alharbi, O. A., Williams, A. T., Phillips, M. R., Thomas, T. (2016): Textural characteristics of sediments along the southern Red Sea coastal areas, Saudi Arabia. Arab. J. Geosci. 9: 735.

Butzer, K. W., Hansen, C. L. (1968): Desert and River in Nubia: Geomorphology and Prehistoric Environments at the Aswan Reservoir. University of Wisconsin Press, Madison, Wisconsin, 562 p.

Craig, T., Jackson, J., Priestley, K., McKenzie, D. (2011): Earthquake distribution patterns in Africa: their relationship to variations in lithospheric and geological structure, and their rheological implications. Geophys. J. Int. 185: 403-434.

Dawood, Y. H., Abd El Naby, H. H. (2012): Distribution of uranium and thorium radioelements in subsurface Pleistocene-Holocene sediments of the Nile Delta, Egypt. JAKU Earth Sci., 23(2):149-168.

Folk, R. L., Ward, W. C. (1957): Brazos River bar- a study in the significance of grain size parameters. J. Sed. Petrol. 27(1):3-26.

Folk, R. L. (1954): The distinction between grain size and mineral composition in sedimentary nomenclature. J. Geol. 6(4):344-359.

Folk, R. L. (1966): A review of grain size parameters. Sedimentology 6:73-93.

Foucault, A., Stanley, D. J. (1989): Late Quaternary palaeoclimatic oscillations in East Africa recorded by heavy minerals in the Nile delta. Nature 339:44-46.

Friedman, G. M. (1961): Distinction between dune, beach and river sand from their textural characteristics. J. Sed. Petrol. 31(4): 514-529.

Frihy, O. E., Lotfy, M. F. Komar, P. D. (1995): Spatial variations in heavy minerals and patterns of sediment sorting along the Nile Delta, Egypt. Sediment. Geol. 97: 33-41.

Galehouse, J. S. (1971): Point counting. In: Carver, R.E. (ed) Procedures in sedimentary petrology. Jhon Wily Interscience, New York, 385-407.

Garzanti, E., Andò, S., and Vezzoli, G. (2009): Grain-size dependence of sediment composition and environmental bias in provenance studies. Earth Planet. Sci. Lett. 277: 422-432.

Garzanti, E., Andò, S., Limonta, M., Fielding, L., Najman, Y. (2019): Diagenetic control on mineralogical suites in sand, silt, and mud (Cenozoic Nile Delta): Implications for provenance reconstructions. EarthSci. Rev. 185:122-139.

Hassan, F. A. (1976): Heavy Minerals and the Evolution of the Modern Nile. Quat. Res. 6:425-444.

Hubert, J. F. (1962): A zircon-tourmaline-rutile maturity index and the interdependence of the composition of heavy mineral assemblages with the gross composition and texture of sandstones. J. Sed. Petrol. 32: 440-450.

Johnsson, M. J. (1993): The system controlling the composition of clastic sediments. In: Johnsson MJ, Basu A (Eds.), Processes Controlling the Composition of Clastic

Sediments. Geological Society of America, Special Paper 284: 1-19.
Johnsson, M. J., Meade, R. H. (1990): Chemical weathering of fluvial sediments during alluvial storage: the Macuapanim Island point bar, Solimoes River, Brazil. J. Sed. Petrol. 60:827-842.
Lario, J., Spencer, C., Plater, A. J., Zazo, C., Goy, J. L., Dabrio, C. J. (2002): Particle size characterization of Holocene back-barrier sequences from North Atlantic coasts (SW Spain and SE England). Geomorphology, 42: 25-42.
Macgregor, D. S. (2012): The development of the Nile drainage system: integration of onshore and offshore evidence. Pet. Geosci., 18: 417-431.
Mahmoud, A. A. (2018) A guide to the Egyptian sediments, Latvia, European Union, ppt.194.
Mange, M. A. and Maurer, H. W. (1992): Heavy Minerals in Colour. Chapman Hall, London, UK. 147p.
Milner, H. B., Ward, A. M. and Highan, F. (1962): Sedimentary petrography, v.11, principle and application. 4th ed. New York: The Macmillan.
Morton, A. C. and Hallsworth, C. (1994): Identifying provenance-specific features of detrital heavy mineral assemblages in sandstones. Sediment. Geol. 90 (3,4):241-256.
Morton, A. C. (1985): Heavy minerals in provenance studies. In: Provenance of arenites, G.G., Zuffa(Ed.), Dordrecht, Reidel, 249-77.
Mycielska-Dowgiałło, E. and Ludwikowska-Kędzia M. (2011): Alternative interpretations of grain-size data from quaternary deposits. Geologos 17(4):189-203.
Nechaev, V. P. and Isphording, W. C. (1993): Heavy-mineral assemblages of continental margins as indicators of plate-tectonic environments. J. Sed. Petrol. 63: 1110-1117.
Pettijohn F. J. (1941): Persistance of heavy minerals and geologic age. J. Geol. 49:610-625.
Pettijohn F. J. (1975): Sedimentary rocks. 3rd .Edition, Harper & Row Publ., 628 p.
Said, R. (1981): The Geological Evolution of the River Nile: Springer-Verlag Inc, New York, 151 p.
Said, R. (1993): The River Nile: Geology, Hydrology and Utilization. Pegamon Press, Oxford, 320 p.
Salem, R. (1976): Evolution of Eocene–Miocene sedimentation patterns in parts of Northern Egypt. AAPG Bull. 60:34-64.
Savage and Potter. (1991): Petrology of modern sands of the Rios Guaviare and Inirida, southern Colombia: tropical climate and sand composition. J. Geol. 99:289-298.
Shukri, N. M. (1950): The mineralogy of some Nile sediments. Quart. Jour. Geol. Soc. London, 105:511- 534.
Siegel, F. R., Gupta, N., Shergill, B., Stanley, D. J. and Gerber, C. (1995): Geochemistry of Holocene sediments from the nile delta. J. Coast. Res. 11(2):415-431.
Stanley, D. J. and Wingerath, J. G. (1996): Clay mineral distributions to interpret Nile Cell provenance and dispersal: I. Lower River Nile to Delta sector. J. Coast. Res. 12:911-929.
Weltje, G. J., and von Eynatten, H. (2004): Quantitative provenance analysis of sediments: review and outlook. Sediment. Geol. 171: 1-11.

Wendorf, F. and Schild, R. (1976): Prehistory of the Nile Valley. Academic Press, London, 404 p.
Wong, F. L. (2002): Heavy mineral provinces of Palos Verdes margin, southern California. Cont. Shelf Res. 22: 899–910.